Thermal behaviour of magnetron sputtered tungsten and tungsten-boride thin films

Liga Avotina
Institute of Chemical Physics
University of Latvia
Riga, Latvia
ORCID: 0000-0001-5197-4196

Lada Bumbure
Institute of Biomedical Engineering and Nanotechnologies
Riga Technical University
Riga, Latvia
ORCID: 0000-0001-9860-6956

Annija Elizabete Goldmane
Institute of Chemical Physics
University of Latvia
Riga, Latvia
ORCID: 0000-0001-9118-1043

Edgars Vanags
Institute of Solid State Physics
University of Latvia
Riga, Latvia
email: edgars.vanags@cfi.lu.lv

Marina Romanova
Institute of Biomedical Engineering and Nanotechnologies
Riga Technical University
Riga, Latvia
ORCID: 0000-0003-2556-0170

Hermanis Sorokins
Institute of Biomedical Engineering and Nanotechnologies
Riga Technical University
Riga, Latvia
email: Hermanis.Sorokins@rtu.lv

Aleksandrs Zaslavskis
Joint-stock company "ALFA RPAR"
Riga, Latvia
email: alfa@alfarzpp.lv

Gunta Kizane
Institute of Chemical Physics
University of Latvia
Riga, Latvia
ORCID: 0000-0002-3206-5322

Yuri Dekhtyar
Institute of Biomedical Engineering and Nanotechnologies
Riga Technical University
Riga, Latvia
ORCID: 0000-0001-8262-0438

2022 International Conference on Applied Electronics (AE) | 978-1-6654-9482-3/22/$31.00 ©2022 IEEE | DOI: 10.1109/AE54730.2022.9920033

***Abstract*— Magnetron sputtered tungsten and tungsten diboride nanofilms are proposed to be used in microelectronic devices. Methods of deposition for nanofilms on oxidized silicon followed by etching is among the techniques to be applied for production. However, physical-chemical interactions between various films need to be taken into account. Therefore, a complete surface and in-depth characterization of synthesized films is necessary. Tungsten and tungsten diboride nanofilms are deposited by magnetron sputtering technique, followed by plasma chemical and chemical etching. Characterization of the structures is separated in several main steps including surface morphology, analysis of element composition as well as characterization of thermal properties, including estimation of presence of thermally active emission centers and thermally induced chemical conversions.**

Keywords*— *tungsten, tungsten diboride, nanofilms, thermal treatment, thermally stimulated exoelectron emission

I. Introduction

Tungsten (W) is widely used in various fields of application, such as micro- and nanoelectronics [1], in contacts, interconnections [2] as well as for fabrication of protective coatings for turbine blades in aeronautical engines [3] for plasma facing components in nuclear reactors [4]. Various deposition techniques, such as electron beam, arc deposition, pulsed laser deposition, molecular beam epitaxy, high-pressure torsion [5], plasma sputtering [6] can be used for production of W thin films with targeted crystalline structure, physical and chemical properties. High power impulse magnetron sputtering can be applied for fabrication of hard W coatings, up to 32.2 GPa. [7], while magnetron sputtering with low pressure and elevated temperature allows to produce low-resistivity polycrystalline W films [8]. Magnetron sputtering at gas pressure above 5 mTorr and power less than 40 watts results in forming β-W phase, because of the reduced energy from the deposited atoms [9]. Varying substrate bias, magnetron power and deposition pressure it is possible to achieve promotion of either α-W or β-W phase deposition [10]. Challenging part for W deposition is, that formation of either α- or β- phase is influenced also by the substrate type [11]. By adding additional variable to the deposition process, such as introducing presence of other elements, like boron (B), films with elevated hardness can be achieved [12]. The number of multiple variables causes a necessity for characterization of structure, element distribution and thermal properties of magnetron sputtered thin films for application in microelectronics.

In this research thermostability in a range of +20 °C to +600 °C of the W and tungsten-boron (WxBy) nanofilms produced by magnetron sputtering technique was analysed. For this exoemission and thermogravimetry measurements that indicate presence of heat induced phase transitions were employed.

II. Experimental

Magnetron sputtered thin W and WxBy thin films were deposited on oxidized Si substrates. Deposited films were characterized by means of infrared spectrometry, scanning electron microscopy (SEM), energy dispersion X-ray spectrometry (EDX) and diffractometry as well as exoemission spectrometry.

A. Samples and preparation

W and WxBy films with thickness of 150 nm were fabricated by a magnetron sputtering technique. The fabrication was performed by a joint stock company "ALFA RPAR". Si (111) wafers with diameter of 76 mm were used for fabrication of films. Prior magnetron sputtering, Si substrates were cleaned by using Caro's acid. Si was heated up to 1130 °C in inert atmosphere and at this temperature was thermally grown a SiO_2 layer. On the dioxide W and WxBy nanofilms were deposited and procedure followed by plasma etching. After deposition, the thickness of the films was monitored with means of profilometry. Scheme of created structures is shown in Fig.1. The etched and covered surfaces were analysed by means of spectrometric methods.

978-1-6654-9482-3/22/$31.00 ©2022 IEEE

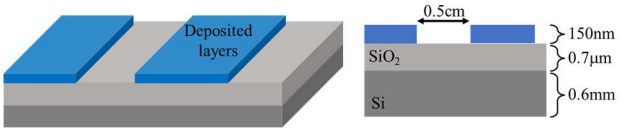

Fig. 1. Scheme of fabricated structures

B. *Methods and instrumentation*

Deposited films were characterized by Fourier transform infrared (FTIR) spectrometer *Bruker Vertex 70v*, equipped with attenuated total reflection module (ATR), spectral range 400-4000 cm^{-1}, resolution ±2 cm^{-1}, in vacuum 2.95 hPa, 20 recoded spectra per measurement, at least 3 measurements per sample, giving at least 60 spectra per sample. For both types of the films a modification by thermal oxidation applied and subsequently FTIR spectra measured. Thermal oxidation modification in details described in [13].

Surface morphology was characterized by SEM; element content – by EDX. The samples were adhered to aluminium stubs using conductive carbon adhesive tape. Afterwards, the morphology and elemental distribution of samples were evaluated by a high-resolution field emission SEM apparatus *Thermo Scientific™ Helios™ 5 UX*. During the measurements, the working distance was set to 4 mm. The SEM images were collected at 2 kV electron acceleration voltage and 25 pA current by detecting secondary electrons using a through-the-lens detector (TLD) and an ion conversion and electron (ICE) detector, while the energy-dispersive X-ray spectroscopy (EDS) was performed at an acceleration voltage of 15 kV.

Photo-thermo stimulated exoelectron emission (PTSEE) spectra of the samples were measured in a vacuum of 10-5 Torr using a spectrometer designed in the laboratory of Riga Technical University. During measurements, the samples were heated from room temperature to 580 °C at a rate of 10 °C/min. The emitted electrons were detected using an SEM-6M secondary electron multiplier (VTC Baspik, Russia) connected to a Robotron 20046 radiometer and a Hamamatsu Photonics M8784 counting board [14, 15].

In parallel, thermal treatment was performed by a thermogravimetry device *SEIKO EXSTAR 6300*, in Al_2O_3 crucibles 5 mm diameter, located on horizontal balance beam system, equipped with Pt/PtRh thermocouple ensuring mass and temperature registration during heating.

III. Results and Discussion

An intercomparison between synthesized 150 nm W and WxBy films performed, comparing surface morphology, chemical bonds as well as exoemission spectra results together with mass change processes. As well as modification method by thermal oxidation was applied for both types of films.

A. *Microstructure analysis*

Microscopy images of W and WxBy films show that the surface of both types of the films is homogeneous. SEM images of edge structures of W and WxBy are in Fig.2 and 3. In the EDX analysis the beam penetration depth is more than 150 nm, therefore the element composition information is for deposited film together with the SiO_2. An example of WxBy film is in Fig.4. The element content analysis on non-modified WxBy film gives the W and B ratio of around 2.3, leading to overall composition of the thin film as WB_2.

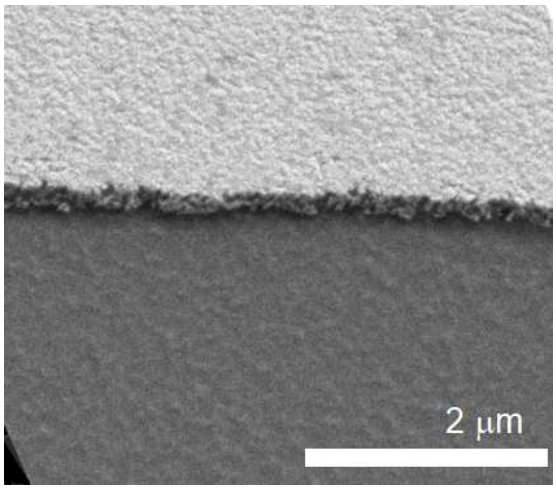

Fig.2 SEM image of W coating on Si-SiO_2

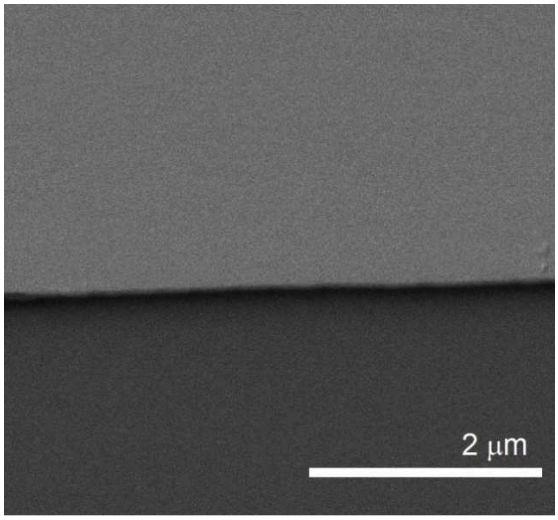

Fig.3. SEM image of WxBy film on Si-SiO_2

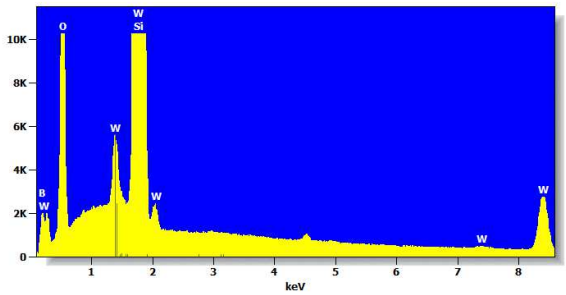

Fig.4. Energy dispersion X-ray spectrum of WxBy film.

For analysis of chemical bonds by the FTIR-ATR a modification method by thermal oxidation was applied, and the modified films further analysed by FTIR. In the spectra of non-modified films, in the etched surfaces Si-O bonds are determined. An example of FTIR spectra of etched are is in Fig.4. By oxidizing W and WxBy films, W-oxygen (O) bonds- W=O and W-O - occur. The polar W-O and W=O can be detected by FTIR and presence of synthesized bonds is used as indicator to determine homogeneity of the film [15]. FTIR spectra of etched areas and thin films prior oxidation are in Fig.5. It can be seen that polar bonds of SiO_2 are clearly visible in the spectra. A peak at 430-480 cm^{-1} could be attributed to Si-O bending vibrations, broad signals are in a region 1015-1135 cm^{-1} are from Si-O-Si as well as from Si-O

[16]. The sputtered films give practically no spectrum, showing that films are homogeneous and completely covering SiO_2.

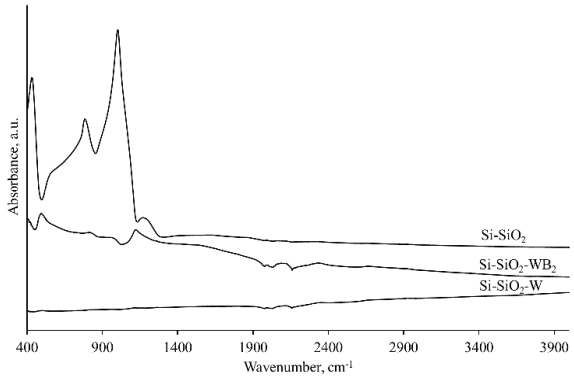

Fig.5. Infrared spectra of thin films and etched areas

Additionally, W and O ratio is determined by EDX and gives result that W is oxidized to the ratio of $WO_{2.9}$, leading to conclusion, that likely mixture of WO_2 and WO_3 oxides are formed. In order to monitor thermal modification, for selected films thermogravimetry results were registered. Thermal exposure to air gives mass increase already above 200 °C, that might be related with sorption of water, CO_2 on the surface followed by complex oxidation process involving presence of water vapour, O_2 and CO_2. Thermogravimetry curves of W and WB_2 thin films are in Fig.6.

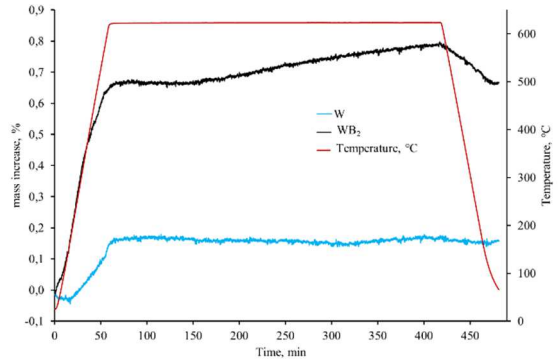

Fig.6. Thermogravimetry curves of W and W_2 films

By exposing the films at the maximal temperature, no additional significant mass or FTIR spectra changes were observed. FTIR spectra of W and WB_2 films exposed to 600 °C for 1, 3 and 6 hours are in Fig.7 and 8 respectively.

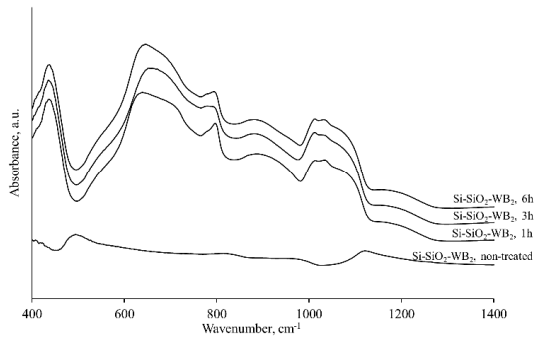

Fig.7. Infrared spectra of WB_2 films - non-modified and treated at 600 °C for 1, 3 and 6 hours.

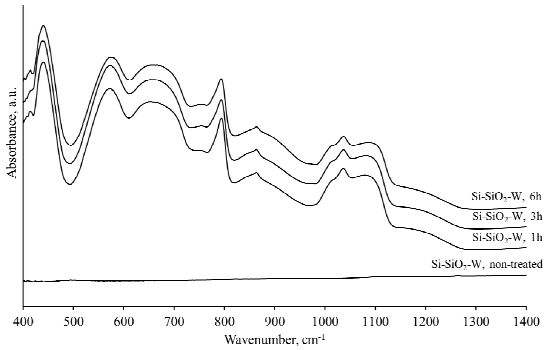

Fig.8. Infrared spectra of W films - non-modified and exposed at 600 °C for 1, 3 and 6 hours.

Comparing thermal behaviour of W and WB_2 films, it can be concluded, that mass gain within the temperature range up to 600 °C shows to mass increase up to 0.6 % from initial mass. For the W films the mass increase reaches around 0.2 % and is related with reaction of films with oxygen. Data can be seen in Fig.9.

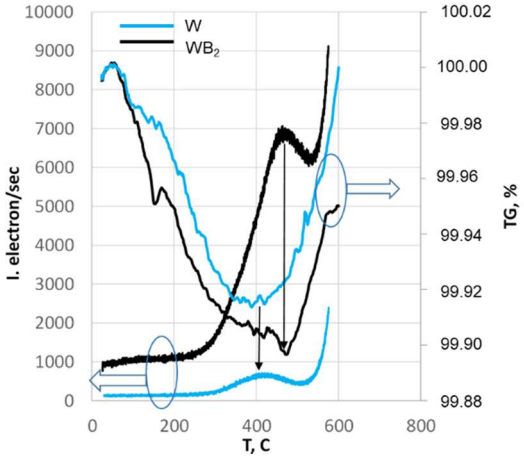

Fig.9. Exoemission and thermogravimetry curves for W and WB_2 films.

TG % measurements demonstrated that both WB_2 and W films have heat induced extremums (minimums) at the temperature range 400-500 °C. These mass changes in oxygen containing environment (air) corelate well with thermally induced exomemission events. The alongside measurements of the PTSEE also demonstrated maximums at the same temperature range. Moreover, the temperatures of the PTSEE maximums and minimums of TG % for W and WB_2 films accordingly are alike. The presence of the PTSEE maximums indicates that the phase transitions [17, 18] took place – for W films around 410 °C and WB_2 films around 485 °C, resulting in 70-80 °C difference, that can be seen Fig.9. The WB_2 films delivered higher electron emission current against W ones, that favour of WB_2 as the more effective emitter of the electrons. Such behaviour may be caused due presence of B heteroatoms and their dislocation in the lattice.

IV. Conclusions

Therefore, one may conclude that heat induces phase transitions both in 150 nm magnetron sputtered W and WB_2 films. However, presence of B in films causes increase of the phase transition temperature for around 70-80 °C in

comparison with pure tungsten films. Phase transitions influence the ability to emit electrons from the films. In fact, the electron emission current at the repeated heating was less compared with the native specimens.

ACKNOWLEDGMENT

The research was supported by the ERDF project No. 1.1.1.1/20/A/109 “Planar field emission microtriode structure”.

REFERENCES

[1] Y. Wang, Q. Tang, D. Chen, X. Liu, J. Yan, X. Xiong, Microstructure and magnetron sputtering properties of tungsten target fabricated by low pressure plasma spraying, International Journal of Refractory Metals and Hard Materials, vol. 87, 2020, 105116, https://doi.org/10.1016/j.ijrmhm.2019.105116.

[2] K. A. Gesheva, T. A. Krisov, U.I . Simkov, G. D. Beshkov, Deposition and study of CVD—tungsten and molybdenum thin films and their impact on microelectronics technology, Applied Surface Science, vol. 73, 1993, pp. 86-89, https://doi.org/10.1016/0169-4332(93)90150-A.

[3] P. Colpo, T. Meziani, N. Gibson, G. Ceccone and F. Rossi, Tungsten deposition by dual-frequency inductively coupled plasma-assisted CVD. Surface and Coatings Technology, 1999, vol. 116-119, pp. 863–867. doi:10.1016/s0257-8972(99)00223-6

[4] W. Cui, K. Flinders, D. Hancock, P. S. Grant, Joining and cycling performance of ultra-thick tungsten coatings on patterned steel substrates for fusion armour applications,Materials & Design, vol. 212, 2021, 110250, https://doi.org/10.1016/j.matdes.2021.110250.

[5] N. Gordillo, M. Panizo-Laiz, E. Tejado, I. Fernandez-Martinez, A. Rivera, J.Y. Pastor, C. Gómez de Castro, J. del Rio, J.M. Perlado, R. Gonzalez-Arrabal, Morphological and microstructural characterization of nanostructured pure α-phase W coatings on a wide thickness range, Applied Surface Science, vol. 316, 2014, pp. 1-8, https://doi.org/10.1016/j.apsusc.2014.07.061.

[6] E. Vassallo, R. Caniello, M. Canetti, D. Dellasega, M. Passoni, Microstructural characterisation of tungsten coatings deposited using plasma sputtering on Si substrates, Thin Solid Films, vol. 558, 2014, pp. 189-193, https://doi.org/10.1016/j.tsf.2014.03.050.

[7] I.-L. Velicu, V. Tiron, C. Porosnicu, I. Burducea, N. Lupu, G. Stoian, G. Popa, D. Munteanu, Enhanced properties of tungsten thin films deposited with a novel HiPIMS approach, Applied Surface Science, vol. 424, 3, 2017, pp. 397-406, https://doi.org/10.1016/j.apsusc.2017.01.067.

[8] G. K. Rane, S. Menzel, T. Gemming, J. Eckert, Microstructure, electrical resistivity and stresses in sputter deposited W and Mo films and the influence of the interface on bilayer properties, Thin Solid Films, vol. 571, 1, 2014, pp. 1-8, https://doi.org/10.1016/j.tsf.2014.09.034.

[9] A. Kaidatzis, V. Psycharis, K. Mergia, D. Niarchos, Annealing effects on the structural and electrical properties of sputtered tungsten thin films, Thin Solid Films, vol. 619, 2016, pp. 61-67, https://doi.org/10.1016/j.tsf.2016.10.027.

[10] F.T.N. Vüllers, R. Spolenak, Alpha- vs. beta-W nanocrystalline thin films: A comprehensive study of sputter parameters and resulting materials' properties, Thin Solid Films, vol. 577, 2015, pp. 26-34, https://doi.org/10.1016/j.tsf.2015.01.030.

[11] J.-S. Lee, J. Cho, C.-Y. You, Growth and characterization of α and β-phase tungsten films on various substrates, Journal of Vacuum Science & Technology A: Vacuum, Surfaces, and Films, 34(2), 2016, 021502. doi:10.1116/1.4936261

[12] J. Chrzanowska-Giżyńska, P. Denis, S. Woźniacka, L. Kurpaska, Mechanical properties and thermal stability of tungsten boride films deposited by radio frequency magnetron sputtering, Ceramics International, vol. 44, 16, 2018, pp. 19603-19611, https://doi.org/10.1016/j.ceramint.2018.07.208.

[13] A.E. Goldmane, L. Avotina, M. Romanova, A.Muhin, A.Zaslavskis, G. Kizane, Yu. Dekhtyar, “FTIR Analysis of Oxidized Tungsten and Tungsten Diboride Nanolayers,”Materials Science (Medžiagotyra), in press, 2022, doi: 10.5755/j02.ms.29796

[14] M. Romanova, R. Burve, S. Cichon, Yu. Dekhtyar, L. Fekete, D. Jevdokimovs, A. Krumina, K. Palskis, V. Serga, “Effect of Gamma Radiation on Thermostimulated Exoelectron Emission from Gd2O3 Films,”. Nuclear Instruments and Methods in Physics Research Section B: Beam Interactions with Materials and Atoms, vol. 463, pp.21-26, 2020.

[15] M. Romanova, R. Burve, Yu. Dekhtyar, K. Palskis, V. Serga, “Influence of MeV Gamma Photons on Thermally Stimulated Exoelectron Emission from MgO Films,” *Key Engineering Materials*, Vol.903, pp.162-167, 2021.

[16] L. Avotina, E. Pajuste, M. Romanova, A. Zaslavskis, G. Enichek, V. Kinerte, A. Zarins, B. Lescinskis, J. Dehtjars, G. Kizane, FTIR Analysis of Electron Irradiated Single and Multilayer Si3N4 Coatings, Key Engineering Materials, 2018, 788, 96-101, https://doi.org/10.4028/www.scientific.net/KEM.788.96

[17] G. I. Rosenman, Ju. Ja. Tomashpolskii, E. I. Boikova, M. A. Sevostyanov, Exoelectron emission at phase transitions in BaTiO3, Ferroelectrics, 1981, 31:1, 139-142, doi: 10.1080/00150198108201985

[18] V. N. Rudovskii, I. P. Rayevksy, L. M. Rabkin, Exoelectron emission studies of reduced $BaTiO_3$ ceramics, Ferroelecrrics, 1992, Vol. 131, pp. 289-292